
Supporting information for

Full-Visible-Spectrum Emitters from Pyrolysis of Soluble Si-Si Bonded Network Polymers

5

Michiya Fujiki,^{*,†} Yoshiki Kawamoto,[†] Masahiko Kato,[†] Yuji Fujimoto,[†] Tomoki Saito,[†] Shin-ichi Hososhima,[†] and Giseop Kwak^{*,‡}

[†] *Graduate School of Materials Science, Nara Institute of Science and Technology,*

¹⁰ *8916-5 Takayama, Ikoma, Nara 630-0036, Japan, and*

[‡] *Department of Polymer Science, Kyungpook, National UniVersity, 1370 Sankyuk-dong, Buk-gu, Daegu 702-701, Korea*

^{*} Corresponding author. Fax: 81-743-72-6049 (M.F.); 82-53-950-6623 (G.K.).

¹⁵ Tel: 81-743-72-6040 (M.F.); 82-53-9507758 (G.K.). E-mail: fujikim@ms.naist.jp.
(M.F.); gkwak@knu.ac.kr (G.K.).

[†] Nara Institute of Science and Technology.

[‡] Kyungpook National University.

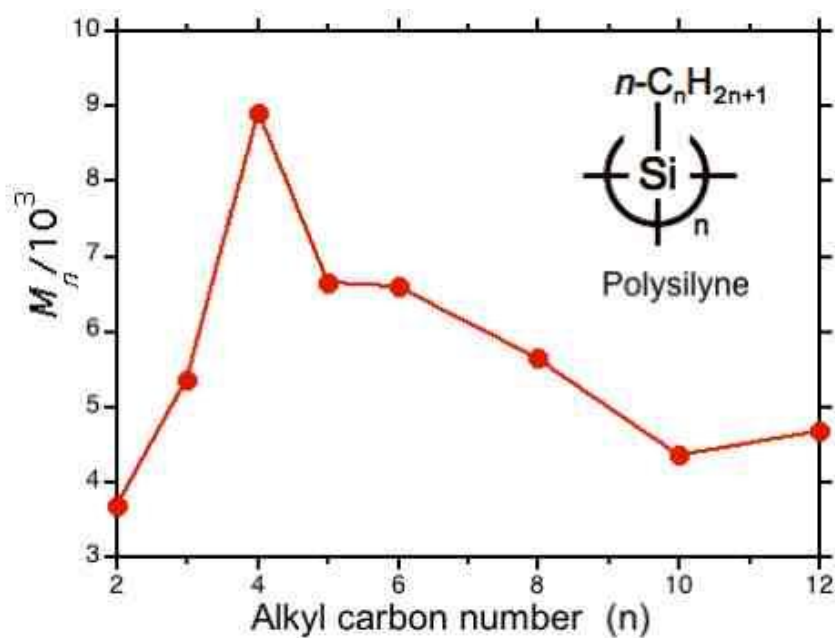


Figure S1. The molecular weights of silicon network polymer (SNP) prepared similarly to n -BSNP. In the case of $\text{CF}_3(\text{CH}_2)_2\text{-SNP}$, n -nonane was used as a polymerization solvent.

5

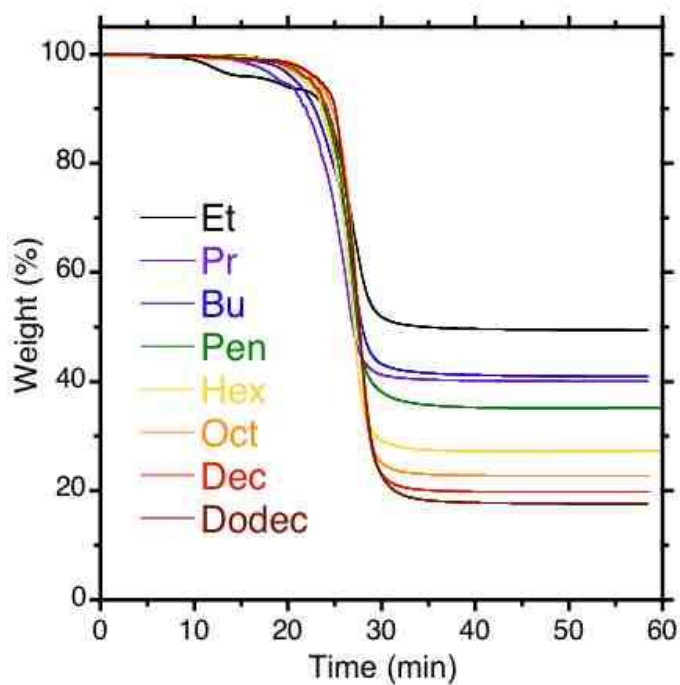
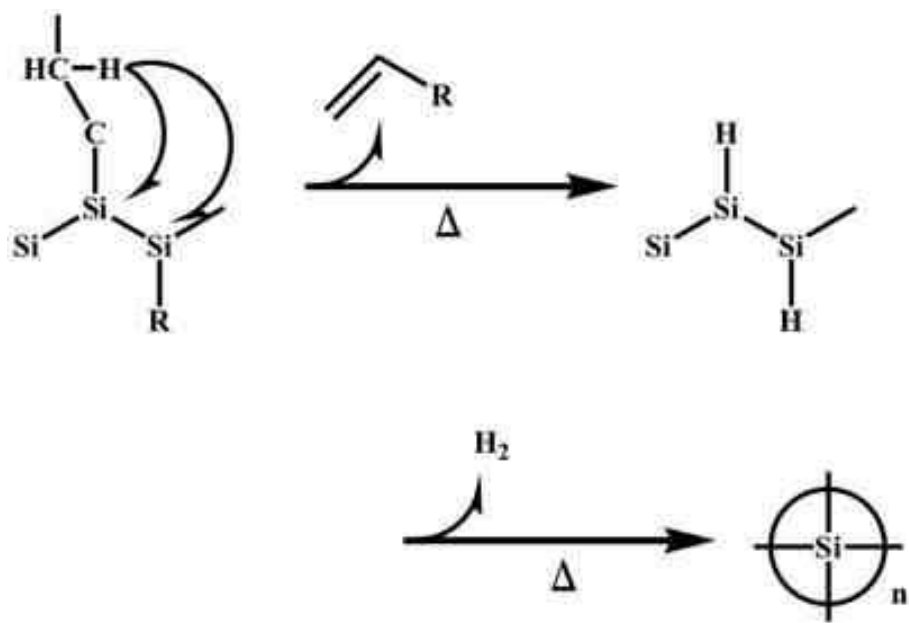
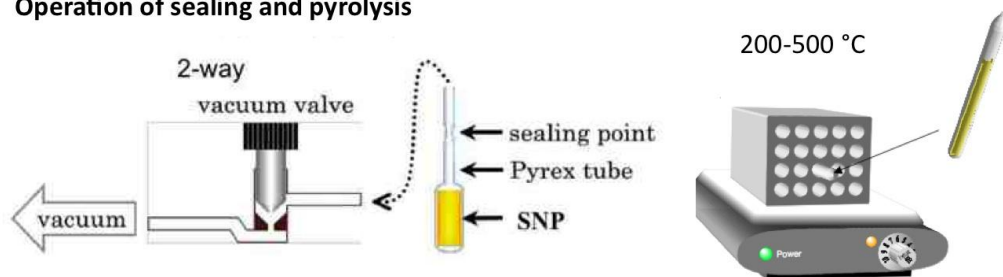


Figure S2. Weight loss data for eight SNPs with different alkyl chains at 500 °C as a function of time in N_2 atmosphere.



Operation of sealing and pyrolysis



5

Figure S1. Mechanism of β -H elimination of SNP and simple apparatus for pyrolysis of SNP in a sealed tube.

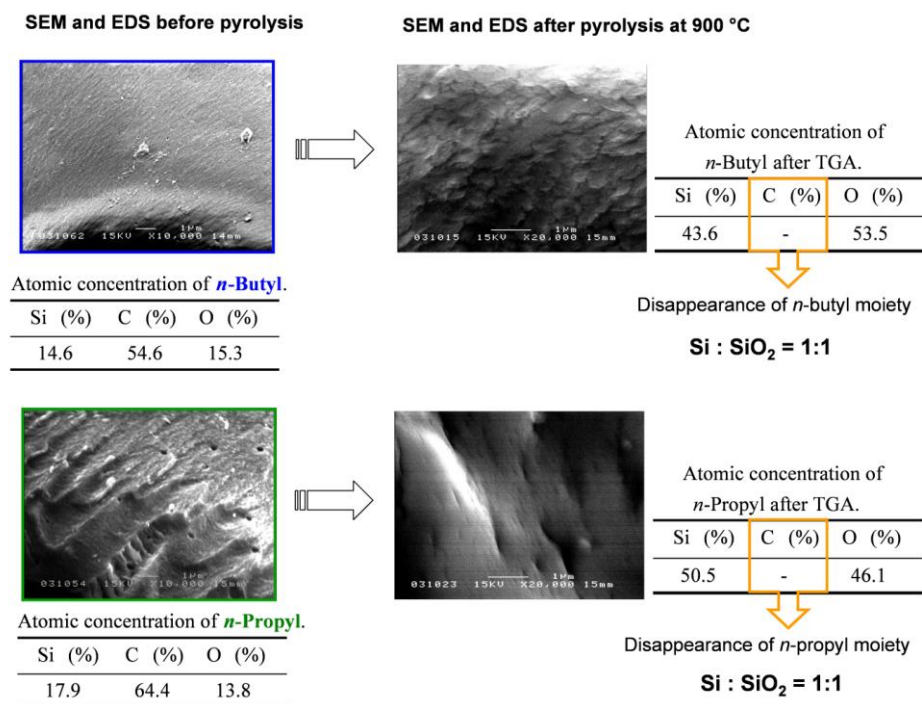


Figure S3. Surface analysis by SEM photographs and EDS of *n*-propyl-SNP and *n*-BSNP before and after pyrolysis at 900 °C.

5

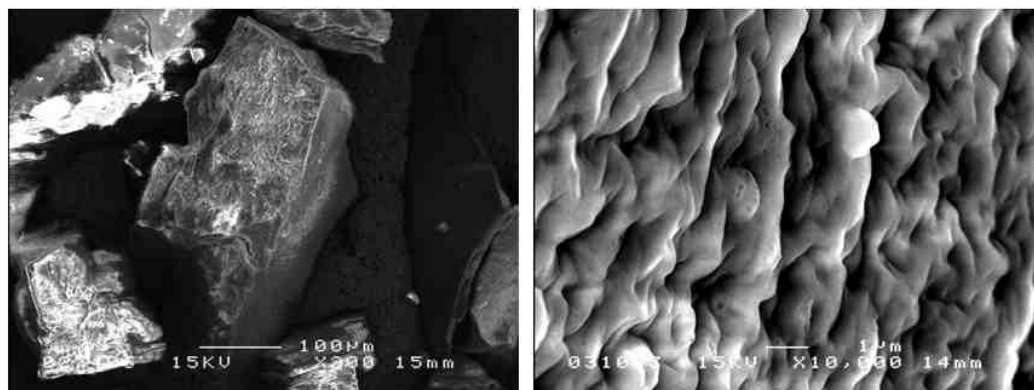


Figure S4. SEM photographs of *n*-propyl-SNP after pyrolysis at 900 °C in N₂ atmosphere.

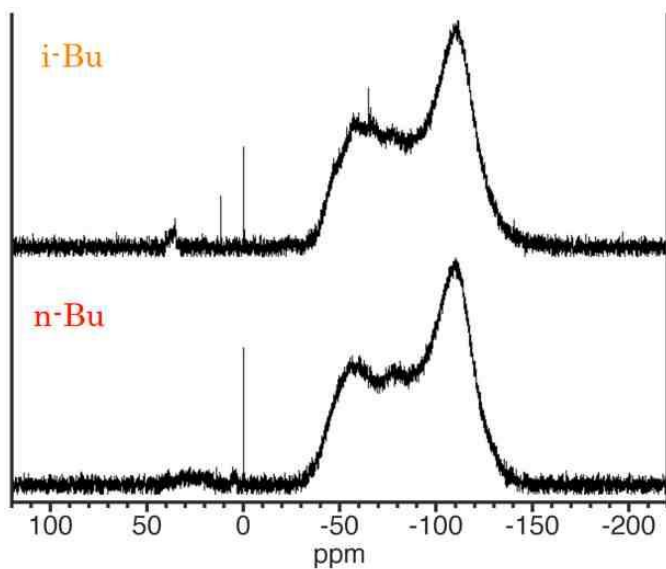


Figure S5. ^{29}Si -FT-NMR of *n*-BSNP and *i*-BSNP (CDCl_3 , 25 °C).

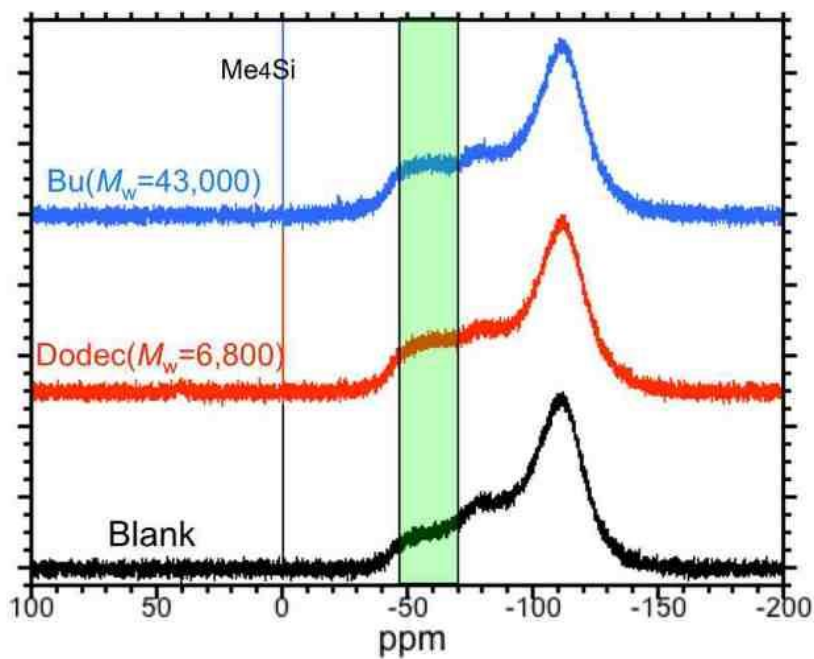


Figure S6. ^{29}Si -NMR of *n*-BSNP and *n*-dodecylSNP (CDCl_3 , 25 °C). A very broad, humped Si-NMR signal around -50 ppm (green bar) implies very limited motion of Si-Si bonded networks. Broad ^{29}Si -NMR signals around -50, -80 ppm and -110 ppm are due to the glass of the NMR tube and probe.

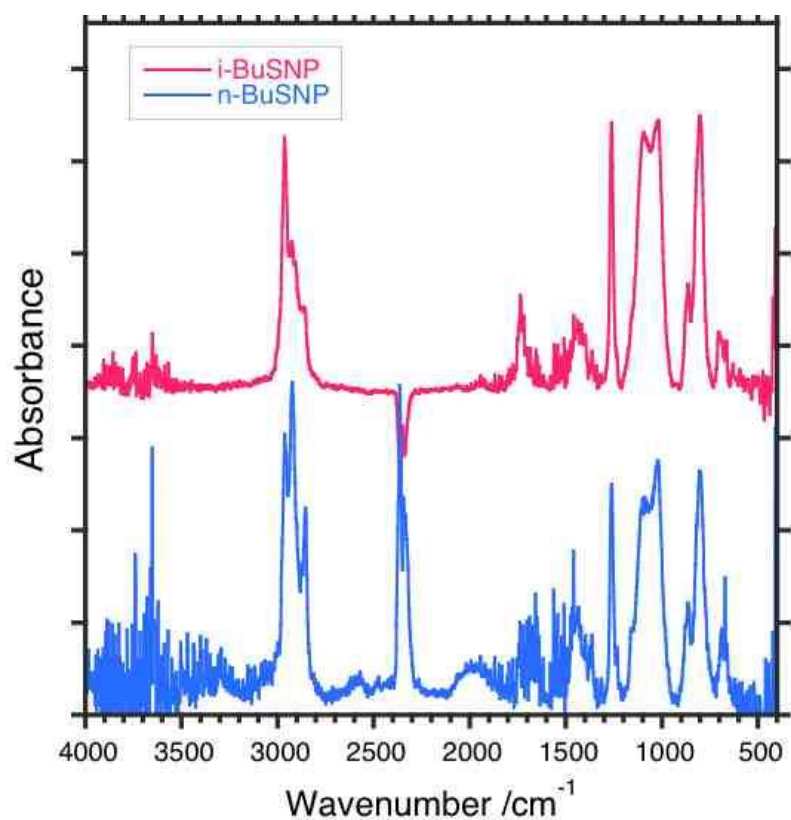


Figure S7. FT-IR spectra of *n*-BSNP and *i*-BSNP cast on a KBr plate.

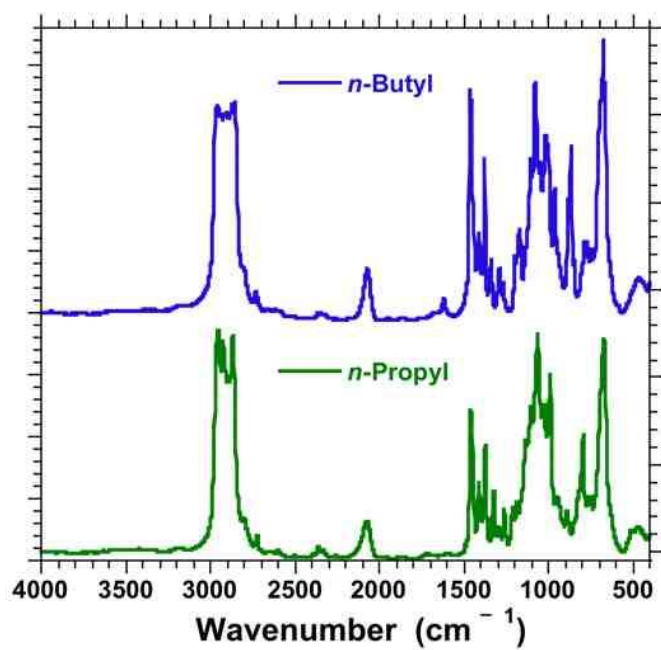


Figure S8. FT-IR spectra of *n*-BSNP and *n*-propyl SNP on a KBr plate.

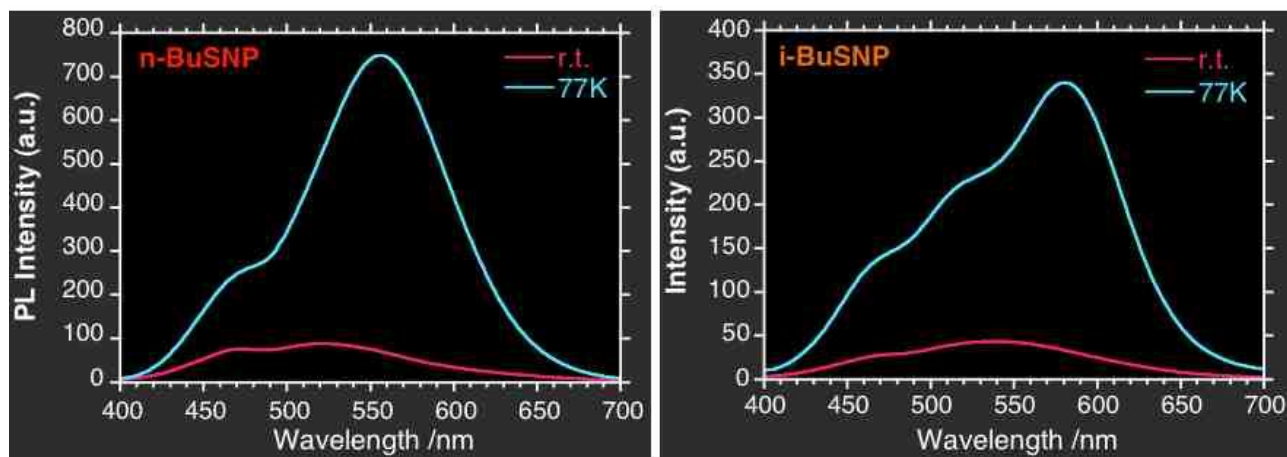


Figure S9. Change in PL intensity (under 360 nm excitation). Left, virgin *n*-BSNP film at 77 K and room temperature; right, *i*-BSNP film at 77 K and room temperature.

5

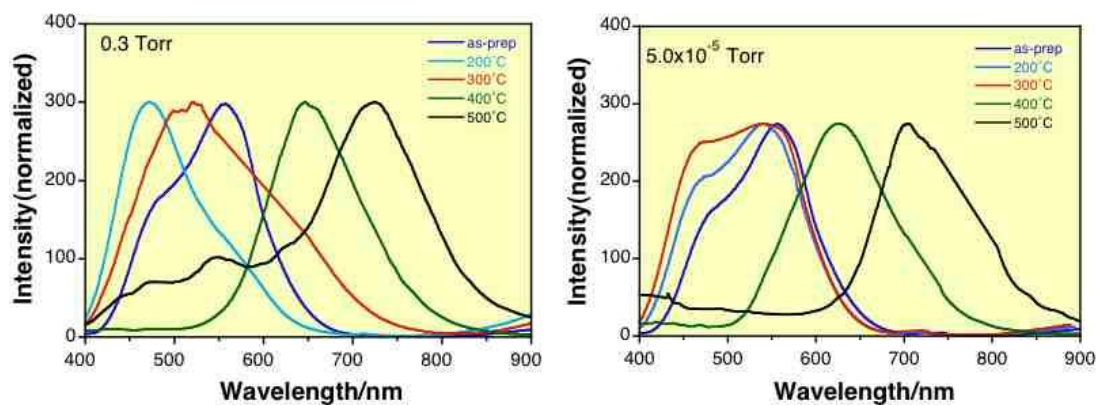


Figure S10. A comparison of PL spectra of *n*-BSNP treated with five different temperatures in two
10 different vacuum conditions: Left at $\sim 3 \times 10^{-1}$ Torr and right at $\sim 5 \times 10^{-5}$ Torr.

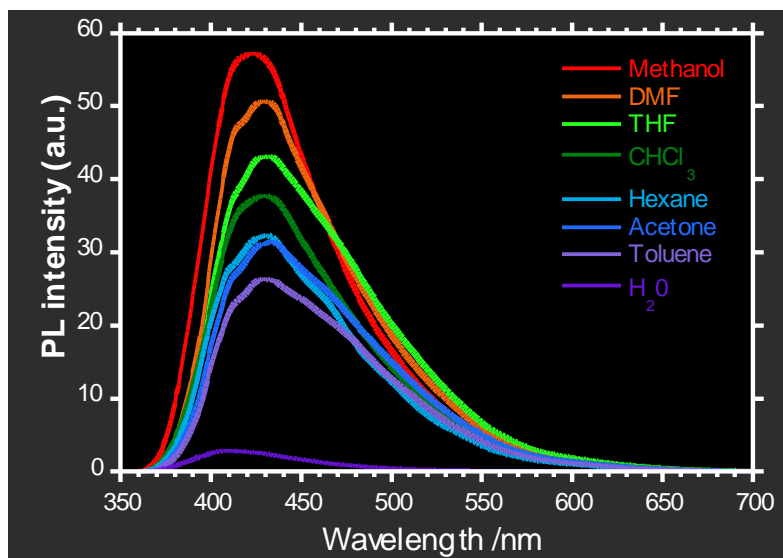


Figure S11. Change in PL intensity of the air-exposed *nc*-Si particles dispersed in solvent: from top to bottom, dimethylformamide, methanol, tetrahydrofuran, chloroform, toluene, acetone, and water.

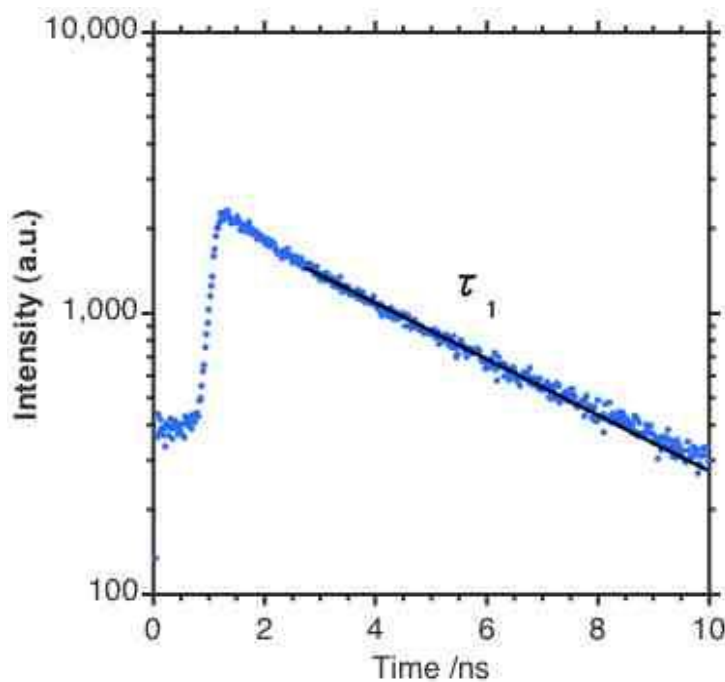


Figure S12. PL decay curve monitored at 560–640 nm (excited at 370 nm, 0.5 mW, pulse width 3 nm, pulse duration 10 nsec) of the air-exposed *nc*-Si particles (pyrolyzed at 500 °C, 90 min) dispersed in *n*-hexane at room temperature.

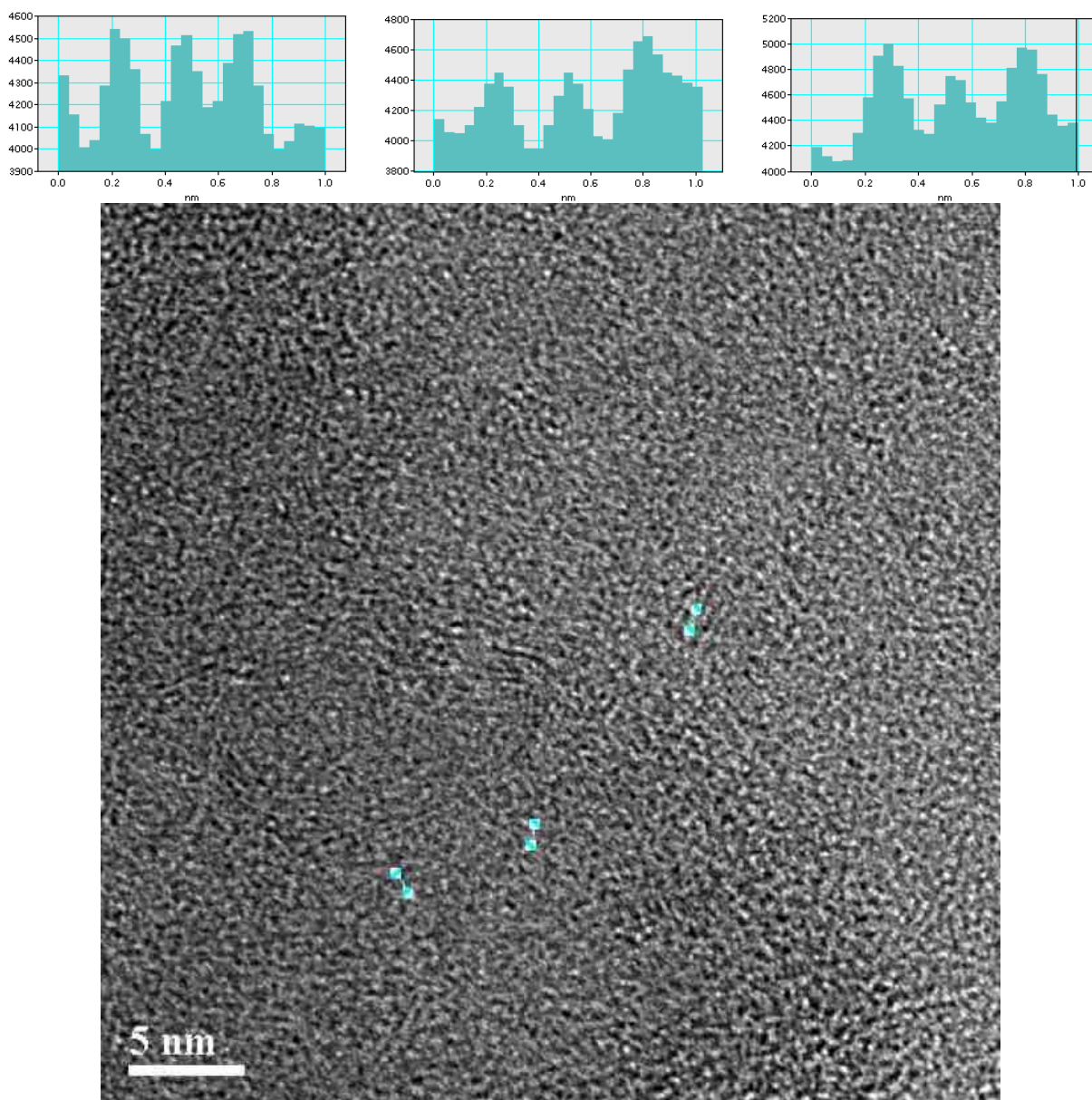


Figure S13. A highly magnified HRTEM image of the air-exposed *nc*-Si particles (the major portions may be ultrafine particles ~ 1 nm). (All plots surface profiles in locations indicated on HRTEM images).

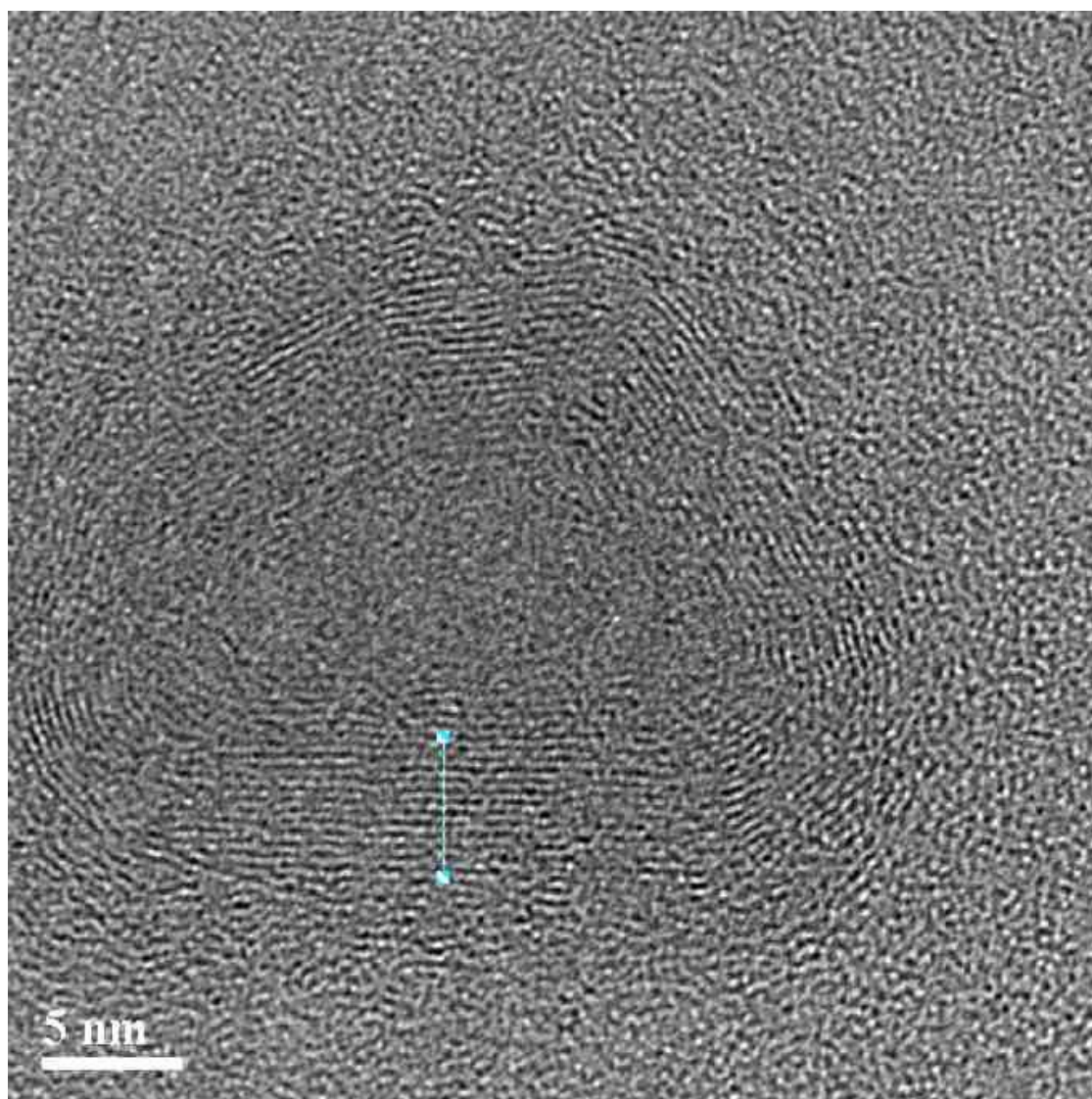
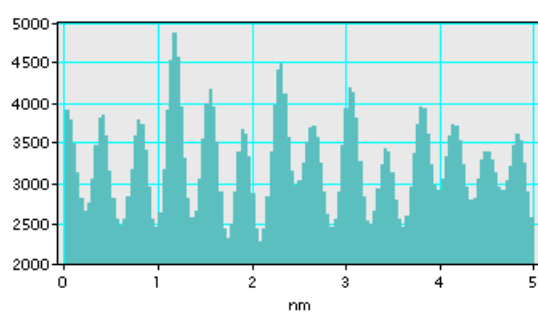


Figure S14. A highly magnified HRTEM image of the air-exposed *nc*-Si particles (baum-küchen-like, multi-layered structures, circular shapes with ~ 0.34 nm spacing). (Surface profile at indicated location).

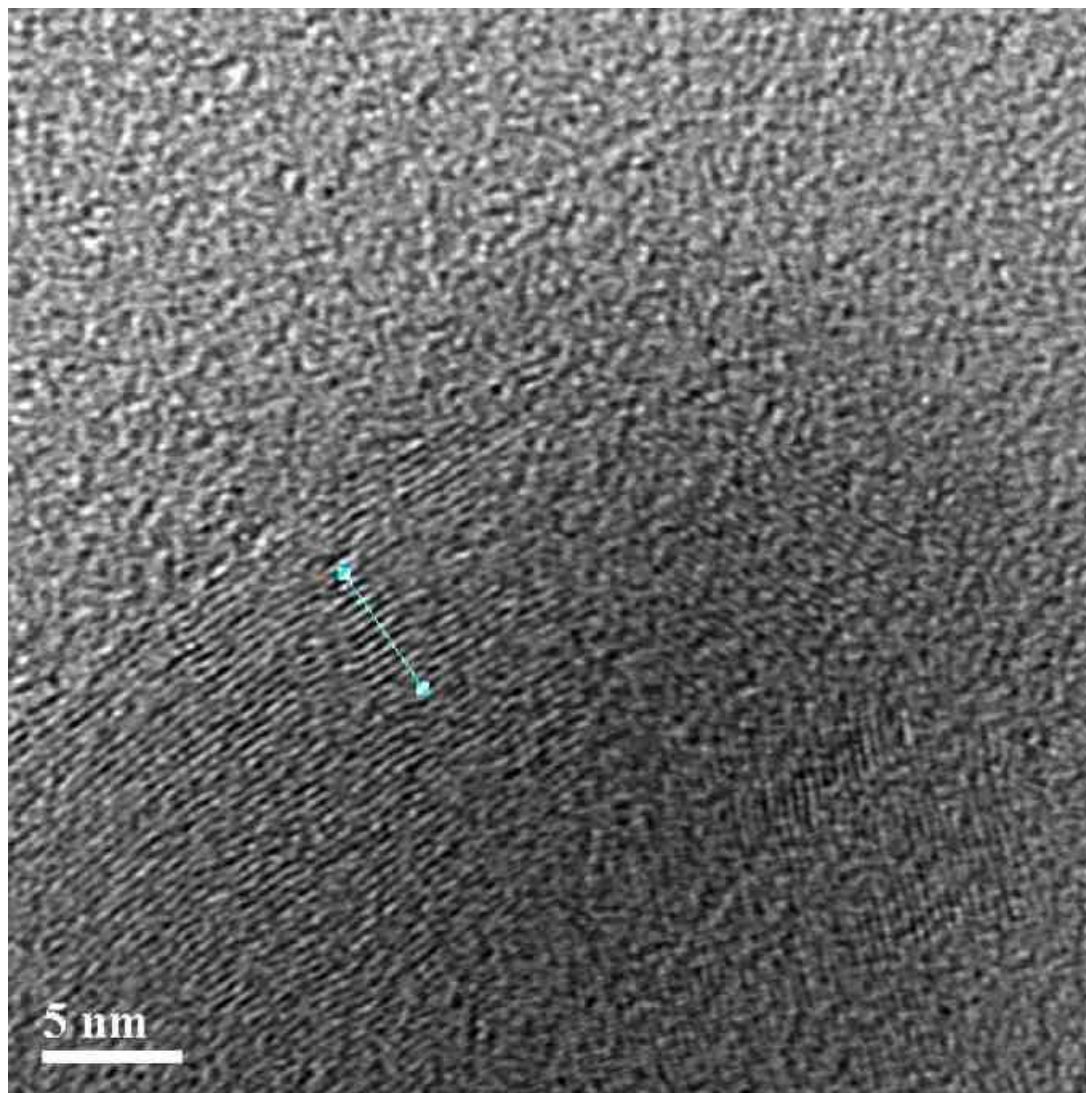
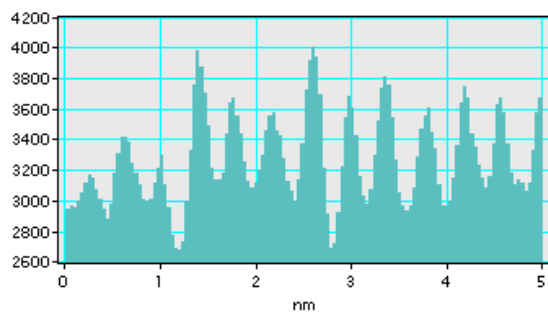
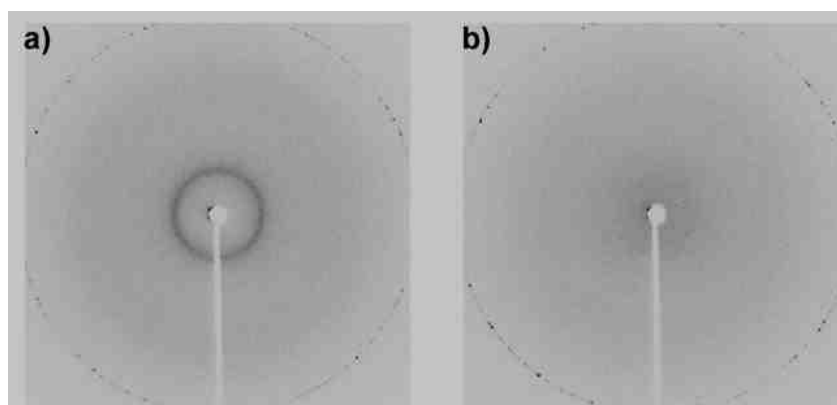
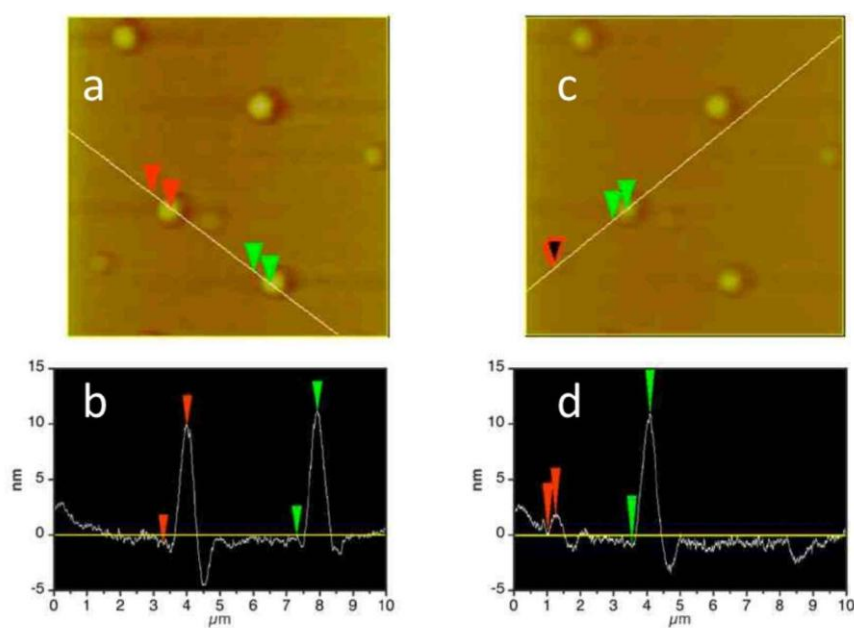


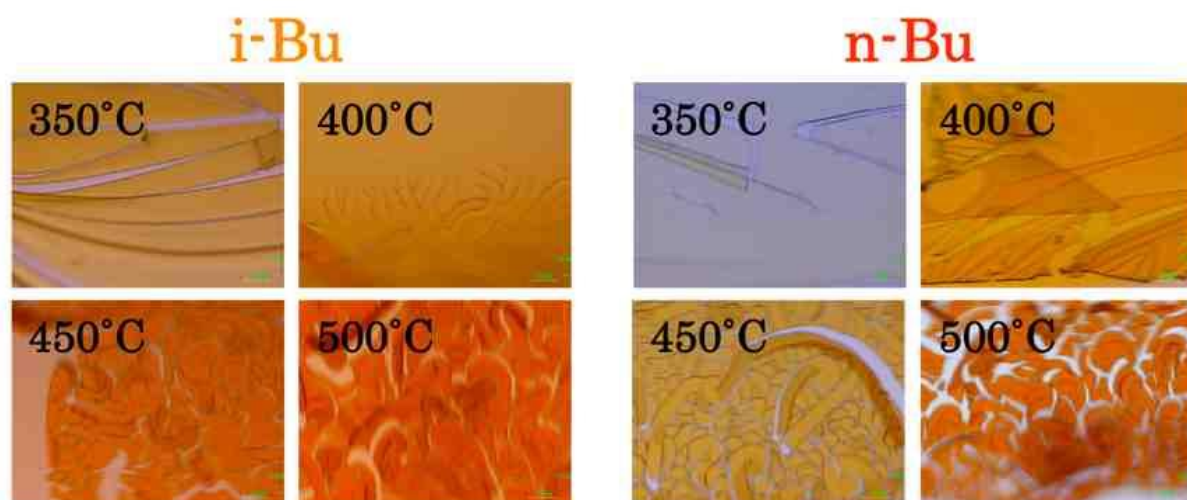
Figure S15. A highly magnified HRTEM image of the air-exposed nc-Si particles (baum-küchen-like, multi-layered structures, lamellar shapes with ~ 0.37 nm spacing). (Surface profiles at indicated location).



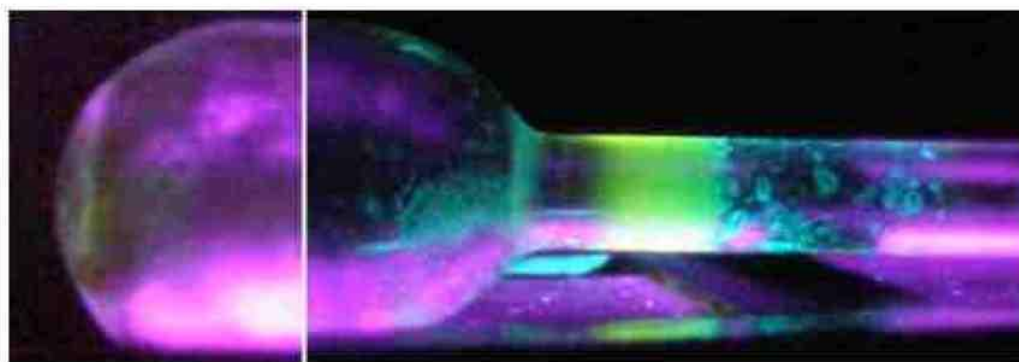
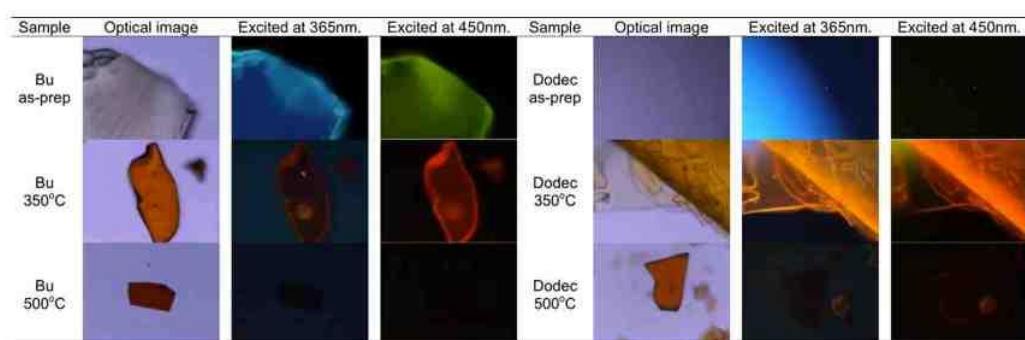
Figures S15a–b. Two-dimensional WAXD images of *n*-BSNP: a, before pyrolysis; b, after pyrolysis.



Figures S16. a–b. AFM images of the particles deposited on mica with several sizes of flat ring disk shapes, ranging from 1.5 to 10 nm in height and from 0.5 to 1 μm in diameter: **b–d.** Cross-section profiles of a and c, respectively.



Figures S17. Optical microscope (OM) images of *n*-BSNP and *i*-BSNP pyrolyzed at 350, 400, 450, 500 °C, indicating formation of macroscopically curved cracks as temperature increases.



Figures S18. Top, FOM images (x 40 magnification) of the pyrolysis samples of *n*-BSNP (top left) and *n*-dodecyl-SNP (top right) at 350 and 500 °C excited at 365 and 450 nm with exposure to air. Bottom, bright visible light emissions from the pyrolytic products of *n*-BSNP deposited onto the inner wall of a sealed quartz tube excited at 365 nm at room temperature.

Table S1. Molecular weights of soluble SNPs.^a

Sample	$M_n \times 10^{-4}$	$M_w \times 10^{-3}$	PDI	Yield (%)
EtSNP	3.7	10.2	2.78	undetermined
<i>n</i> -PrSNP	5.4	18.7	3.49	37
<i>n</i> -BuSNP (<i>n</i> -BSNP)	8.9	42.4	4.75	39
<i>n</i> -PenSNP	6.6	17.5		undetermined
<i>n</i> -HexSNP	6.6	19.8	3.00	undetermined
<i>n</i> -OctSNP	5.7	13.9	2.46	undetermined
<i>n</i> -DecSNP	4.4	7.7	1.75	undetermined
<i>n</i> -Dodec-SNP	4.7	6.8	1.45	undetermined
<i>i</i> -BuSNP (<i>i</i> -BSNP)	2.4	4.0	1.67	18
CF ₃ (CH ₂) ₂ -SNP (FPSNP)	2.8	3.1	1.10	undetermined

^a Calibrated against polystyrene standards.